A&A manuscript no.
(will be inserted by hand later)

Your thesaurus codes are:

ASTRONOMY AND ASTROPHYSICS

April 22, 2002

New UBVRI color distributions in E-type galaxies

II. Central and mean metallicities *

T.P. Idiart[1,3], R. Michard[2], and J.A. de Freitas Pacheco[1]

[1] Observatoire de la Côte d'Azur, B.P.4229, F-06304 Nice Cedex 4, France e-mail: pacheco@obs-nice.fr
[2] Observatoire de Paris, LERMA, 77 Av. Denfert-Rochereau, F-75015, Paris, France e-mail: rmichard@obspm.fr
[3] Instituto de Astronomia, Geofísica e Ciências Atmosféricas Depto. de Astronomia, Universidade de São Paulo, Av. Miguel Stefano, 4200-CEP 04301-904, S. Paulo, SP-Brazil e-mail: thais@iagusp.usp.br

Received date; accepted date

Abstract. Central and mean metallicities are calculated for a sample of 40 early-type galaxies, whose color gradients were reported in a previous paper (Idiart et al. 2002). The present color-metallicity calibration was derived from a grid of evolutionary models which fit the color-magnitude sequence of ellipticals in Coma and Virgo clusters. The mean metallicity gradient derived from our data is $(\Delta[\mathrm{Fe/H}]/\Delta\log r)$ = -0.26±0.08 and the mean sample average metallicity is $<$ [Fe/H] $>$ = 0.01±0.11 (rmsd). Central and mean metallicities are correlated with the central dispersion velocity, consistent with the interpretation by metallicity variations of the color-magnitude sequence and of color gradients. Age effects are also discussed, in particular concerning the interpretation of the Hβ line strength in those objects.

Key words: galaxies: ellipticals and lenticulars, chemical abundances,
metallicity gradients

1. Introduction

The integrated properties of early-type galaxies are linked to the chemical and dynamical evolution of their stellar populations. The integrated colors of ellipticals become redder as the luminosity increases (Visvanathan & Sandage 1977) and the strength of the $\mathrm{Mg_2}$ index correlates well with the central velocity dispersion (Terlevich et al. 1981; Idiart et al. 1996). These relations can be understood if brighter galaxies have higher metallicities. However, this interpretation is still a matter of debate in the literature. Worthey (1996) pointed out that the color-magnitude relation (CMR) can equally be explained by a progressive increase of the stellar population age towards the more luminous galaxies. This alternative is based on a sequence of colors and line strengths computed by adopting *single stellar population* (SSP) models, which are necessarily characterized by a definite age and metallicity. Using colors and spectral indices derived from evolutionary models of ellipticals, including gas inflow and outflow, Bressan et al. (1996) concluded that E-galaxies do not follow a pure sequence either of age or metallicity, with objects of different masses having suffered different star formation histories in spite of having rather old (13-15 Gyr) stellar populations. Kodama & Arimoto (1997) tried to solve the so-called age-metallicity degeneracy by building up two model sequences (age and metallicity sequences), which are normalized to reproduce the CMR of ellipticals in the Coma cluster. They compared the evolution of both CMR sequences up to redshifts z $\sim$ 1 and concluded that the age sequence deviates significantly from observations already at z$\sim$ 0.3, supporting the view that the CMR is primarily a metallicity variation with luminosity. A similar conclusion was reached by Tamura et al. (2000) from the analysis of ellipticals in the Hubble "deep-field", as well as by Saglia et al. (2000), who also study the evolution of color gradients with the redshift.

If these last studies favor the interpretation of the CMR as a "metallicity sequence", the age-metallicity degeneracy still persists in the interpretation of color gradients across E-galaxies. Early-type galaxies tend to be redder in the central regions (Franx et al. 1989; Peletier et al. 1990; Goudfrooij et al. 1994; Michard 1998a, 1998b, 2000), probably due to the presence of a *negative* metallicity gradient along the radius. This interpretation is corroborated by spectroscopic observations indicating generally *negative* line strength gradients in ellipticals (Faber 1977; Davidge 1992; Carollo et al. 1993; Davies et al. 1993; Fisher et al. 1995), except Hβ, which displays a *positive* gradient in most of the cases. Tantalo et al. (1998) found, however, that the nuclear region of some E-galaxies are not only metal-rich but have also a stellar population younger than the outer zones, raising again the question of pos-

Send offprint requests to: J.A. de Freitas Pacheco

* Based partially on data collected at the Observatory of Haute-Provence

sible age differences among stellar populations along the radius.

Radial metallicity gradients can be explained by the dissipative collapse picture. The very first hydrodynamical calculations by Larson (1974, 1975) gave $\Delta[\mathrm{Fe/H}]/\Delta\log r$ ranging from -0.35 up to -1.0, while N-body simulations (Carlberg 1984) suggest values around -0.5. These predictions are "steeper" than those derived from colors and line strength gradients, which are typically about -0.3 dex per decade. However, E-galaxies formed in a pure merging picture should have a very flat gradient, since merging events tend to erase any pre-existing gradient (White 1980).

The conversion of color or line strength gradients into mean metallicities or/and mean population ages requires the use of high quality data. In the present work, central and mean metallicities are derived for a sample of 40 early-type galaxies, whose UBVRI colors and gradients were reported in a preceding paper (Idiart et al. 2002, hereafter Paper I). We believe that the present data have an accuracy adequate for our purposes, since a special care has been taken to improve corrections due to residual background effects, the PSF far wings and "red halo" (for a detailed analysis of these effects, see also Michard 2002). Moreover, color gradients have been calculated in selected ranges, avoiding the central regions of some objects affected by dust. This procedure enables us to obtain by extrapolation reliable colors of the underlying stellar population in the center of the galaxy (see Paper I).

As detailed below, the color-metallicity calibration was derived from evolutionary models, which are expected to take into account the gradual chemical enrichment of the stellar populations. These models have not yet been fully described in a dedicated paper, so that Section 2 is devoted to a summary of their derivation, hopefully sufficient for an understanding of their use in the present contribution. In Section 3 we apply the models to calculations of the average and central metallicities from our color data. In Section 4 various tests of the validity of our results are presented. *A detailed discussion of our evolutionary models, involving various choices of the input parameters, and the corresponding comparisons with colours and other spectral indices, is outside the scope of this paper.* A forthcoming paper will give more details, when the evolution of the spectrophotometric properties as a function of the redshift will be explored.

Often used notations

- r isophotal (or equivalent) radius. $r = (ab)^{1/2}$ for an ellipse of semi-axis a and b.
- $\Delta_{\mathrm{U-V}}$ colour gradient in U−V. $\Delta_{\mathrm{U-V}} = \mathrm{d(U-V)/d}(\log r)$ and similar for other spectral indices.

2. The color-metallicity calibration

Color gradients discussed in Paper I can be used to estimate the mean metallicities of galaxies, in the same way as any other spectrophotometric index, if an adequate color-metallicity calibration is provided. In general, these calibrations involving colors or spectrophotometric indices, like those defined by the Lick's team (see Faber et al. 1985) are performed by using SSP models. Recently, Kobayashi & Arimoto (1999)(KA99) used SSP models developed by Worthey (1994) and a compilation of line-strength gradients from the literature to compute mean metallicities for a sample of 80 E-galaxies. Trager et al. (2000) (TFWG) used also these SSP models to interpret the chemical history of local ellipticals, but they have included corrections to incorporate non-solar abundance ratios. This particular aspect of the index - metallicity calibration was first raised by Borges et al. (1995), who obtained fitting formulas for indices like $\mathrm{Mg_2}$, NaD, including the explicit dependence on the relative element abundance with respect to iron, in order to avoid the bias, present in any stellar spectral library, introduced by the chemical history of our own galaxy.

SSP models carry with them the so-called "age-metallicity degeneracy" since by definition they depend on both parameters. Age and metallicity effects can be disentangled if different indices are used, and if the considered stellar system is really *single* (de Freitas Pacheco 1997a, 1997b; de Freitas Pacheco et al. 1998). Elliptical galaxies are certainly not single stellar systems. If, on the one hand the age range of the population mix constituting the galaxy is quite narrow (3-4 Gyr), a reason generally invoked to justify the use of SSP models, on the other hand the build up of chemical elements requires successive stellar generations, producing a metallicity spread which is adequately described by population mix models.

The calibration used in the present work was derived from a set of models of elliptical galaxies computed according to the assumptions described by de Freitas Pacheco (1996). For these models, the star formation activity always begins at the same redshift: all galaxies have the same age, i.e. 15 Gyr. The star formation efficiency however, varies among models being an increasing function of galaxy mass. Furthermore, the IMF slope is slightly dependent on mass. The models of various masses accordingly develop stellar populations of different mean ages, chemical compositions and spectral properties.

In our approach, the input parameters were chosen by an iterative procedure in order to reproduce the color-magnitude diagram, U−V against M_V of ellipticals in Coma and Virgo (Bower et al. 1992a, 1992b), a procedure also employed by Kodama & Arimoto (1997) to compute CMR at different redshifts. Evolutionary tracks of the Padova group were used in our computations and the integrated properties of the stellar population could be derived in a self-consistent way, for any power-law representing the

Table 1. Model Properties:
The columns give respectively the model identification (1), the initial mass of the galaxy (2), the star formation efficiency (3), the exponent of the IMF (4), the mass fraction lost by the wind (5), the mean age (6), the mean metallicity (7) and the mean relative abundance ratio [Mg/Fe] (8) of the population mix

Model (1)	M_0 ($M_\odot$) (2)	k (Gyr^{-1}) (3)	γ (4)	f_g (5)	τ_*(Gyr) (6)	< [Fe/H] > (7)	< [Mg/Fe] > (8)
1	2×10^{10}	0.445	2.27	0.201	12.5	-0.248	0.44
2	5×10^{10}	0.510	2.22	0.159	12.6	-0.103	0.47
3	2×10^{11}	0.630	2.14	0.110	12.7	+0.109	0.49
4	7×10^{11}	0.730	2.10	0.079	12.9	+0.213	0.49
5	2×10^{12}	0.835	2.06	0.059	13.0	+0.306	0.50

Table 2. Spectrophotometric Properties
The columns give respectively the model N0. (1), the absolute magnitude in the V-band (2), the U−V, B−V, B−R, V−I colors (3) to (6), the indices Mg_2 (7) and Hβ (8)

N0 (1)	M_v (2)	U-V (3)	B-V (4)	B-R (5)	V-I (6)	Mg_2 (7)	Hβ (8)
1	-18.29	1.192	0.909	1.51	1.28	0.237	2.04
2	-19.20	1.283	0.949	1.57	1.32	0.259	1.94
3	-20.55	1.424	1.007	1.66	1.38	0.286	1.77
4	-21.85	1.553	1.045	1.71	1.41	0.297	1.63
5	-22.92	1.668	1.076	1.75	1.43	0.305	1.52

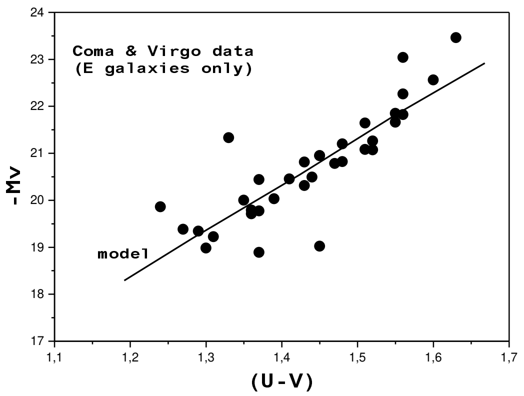

Fig. 1. Color-Magnitude Calibration: the solid line represents the grid of models whose parameters (see text) were adjusted to fit the sequence of data points on Coma and Virgo ellipticals

initial mass function (IMF). Finally the code computes the fluxes in U, B, V, R_c, I_c, K, corresponding color indices, and the Lick indices Mg_2, $< \mathrm{Fe} >= \frac{1}{2}(\mathrm{Fe5270} + \mathrm{Fe5335})$, H$\beta$, NaD and CaT. Note that the colors of SSP used in our synthesis code were computed taking into account effects due to variations of the initial mass function (see below). For the Lick indices, we adopted the calibrations by Borges et al. (1995), including also effects due to the initial mass function.

Figure 1 compares the theoretical color-magnitude diagram with the mentioned data.

The main properties of these models are summarized in Table 1. The second, third and fourth columns are input parameters, namely, the initial mass of the galaxy, the star formation efficiency k (we recall that the star formation rate is proportional to the gas mass, namely, $kM_g(t)$) and the adopted exponent of the IMF ($\gamma = 2.35$ for a Salpeter's law). The following four columns give respectively the mass fraction lost by the galaxy due to the galactic wind, the mean age, the mean metallicity and the mean < [Mg/Fe] > ratio of the stellar population mix. An inspection of Table 1 reveals the two main features of our models: an increasing star formation efficiency and a slightly flatter IMF for more massive galaxies, comparable to the exponent adopted by Tamura et al. (2000) in their models. Both aspects have already been discussed in the literature for the following reasons: the usual "delayed-wind" picture (Matteucci 1994) can explain the observed CMR for ellipticals, if such a relation is interpreted in terms of metallicity variations. However, since this model predicts that the star formation ceases later in more massive galaxies, not only the mean metallicity increases but also the relative contribution of type Ia supernovae, whose ejecta are iron-rich. As a consequence, the relative abundance of the α-elements decreases in the medium, producing a population mix with a decreasing < [Mg/Fe] > ratio, contrary to observations (Matteucci & Tornambè 1987; Matteucci et al., 1998). This problem can be solved either by assuming that massive ellipticals have a higher star formation rate, or by assuming that the more massive E-galaxies have flatter initial mass functions (Matteucci et al. 1998; Chiosi et al. 1998; Tantalo et al. 1998). In fact, we played with both possibilities. Not only higher star formation efficiencies for massive ellipticals are necessary to explain the CMR, but also flatter IMFs, if an adequate representation of data in the Mg_2–< Fe > diagram is equally required. Note that in the extreme case

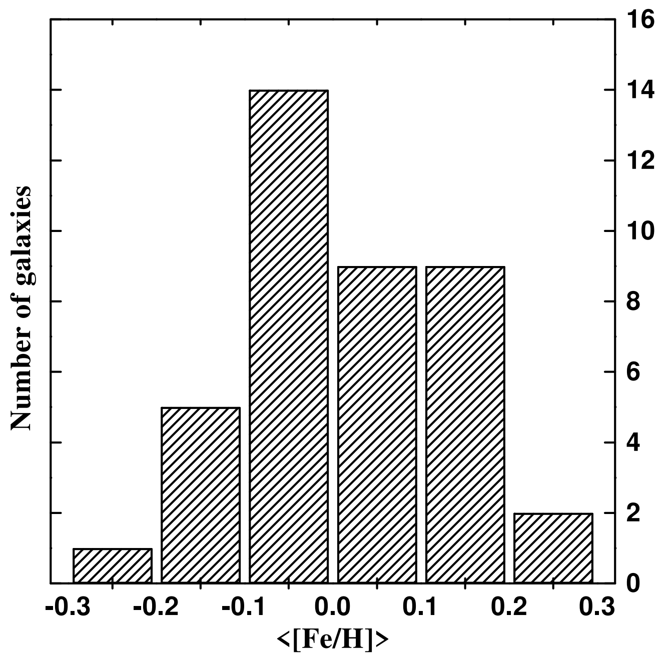

Fig. 2. Distribution of mean metallicities derived from color gradients

(model 5), the required IMF differs only by about 12% from the usual Salpeter's law.

In Table 2 are given some of the spectrophotometric properties which will be used in the present paper.

3. Central and mean metallicities

3.1. Derivation of metallicities from colors

3.1.1. The U−V color

We suppose now that a given (elliptical) shell inside a galaxy, with an equivalent radius r is constituted by a population mix, with a mean age comparable to that of the whole star population of a model galaxy. If, in a first approximation, radial flows and diffusion of stars from one shell to another are neglected, then each shell can be associated to a "one-zone galaxy", characterized by a mean metallicity which reflects the consequences of the star formation activity in this zone. If the observed color gradient is a consequence of a metallicity gradient throughout the galaxy, then it is possible to derive an expression for the latter, using actual data for the former and a theoretical color-metallicity calibration. *In the present computations, we decided to use essentially the U−V color for two reasons: on the one hand, its gradient is large enough to be measured with an accuracy adequate for our purposes; on the other, our models have been constrained to agree with the U−V-luminosity observed relation (Sect. 2).*

In a first approximation, the variation of the U−V color as a function of the radius is given by

$$\mathrm{U-V} = (\mathrm{U-V})_0 + \Delta_{\mathrm{U-V}} \cdot \log(r/r_0) \quad (1)$$

where $(U-V)_0$ is the color at the reference radius r_0 and $\Delta_{\mathrm{U-V}}$ is the corresponding color gradient. These parameters are given in Paper I, for objects included in our sample. From Tables 1 and 2, one obtains a color-metallicity calibration given by

$$[\mathrm{Fe/H}] = -1.600 + 1.162 \cdot (U-V) \quad (2)$$

These two equations can be combined and one obtains

$$[\mathrm{Fe/H}] = [\mathrm{Fe/H}]_0 + \Delta_{[\mathrm{Fe/H}]} \cdot \log(r/r_0) \quad (3)$$

where $[\mathrm{Fe/H}]_0 = -1.600 + 1.162 \cdot (U-V)_0$ is the metallicity at the reference radius, and the resulting metallicity gradient is $\Delta_{[\mathrm{Fe/H}]} = 1.162 \cdot \Delta_{\mathrm{U-V}}$. It is worth mentioning that from our data, the sample average gradient is $\Delta_{\mathrm{U-V}}$ = -0.228±0.068 (rmsd), which is equivalent to a mean metallicity gradient $\Delta_{[\mathrm{Fe/H}]} = -0.26\pm0.08$. A similar exercise with the gradient in the B−R color gives a mean metallicity gradient of -0.22 dex per decade, fully compatible with the result derived from the U−V color.

In order to compute the mean metallicity of the galaxy, the luminous weight of each shell must be introduced. Since the mass-to-luminosity ratio is also derived for each model of galaxy, it is also possible to compute an average metallicity weighted by the mass of the shell. Differences between both procedures are small, in agreement with other authors who have performed similar calculations (Yoshii & Arimoto 1987; Gibson 1997). Here the light weighted average is adopted since this definition corresponds better to what is observed. We assume that the light distribution along the radius can be represented by a de Vaucouleurs' law, namely,

$$I(r) = I_0 e^{-\beta r^{1/4}} \quad (4)$$

In this equation, the parameter I_0 is chosen adequately to normalize the light intensity in the interval r_1, r_2 and the parameter β is related to the effective radius (half-light) R_{eff} of the galaxy by $\beta = (3453/R_{eff})^{1/4}$. The effective radius (B color) used in our computations is given in the fifth column of Table 3 (in arcsec) and was obtained from the RC3, readable directly from the CDS-Strasbourg. Under these conditions, the mean metallicity is

$$<[\mathrm{Fe/H}]> = \log \int_{r_1}^{r_2} 2\pi r I(r) 10^{[\mathrm{Fe/H}]} dr \quad (5)$$

where the integration limits were taken respectively equal to $r_1 = 1.5$" and $r_2 = 2R_{eff}$. The resulting mean metallicities are given in the second column of Table 3 and the third column gives the central metallicity computed at r_1 (see Paper I concerning the adopted definitions of central colors).

Table 3. Central and Mean Metallicities
The columns give respectively the galaxy identification (1), the mean metallicity (2), the central metallicity from colors (3), the central metallicity from Mg_2 indices (4), the effective radius in arcsec (5) and the log of the central velocity dispersion (6)

NGC (1)	$<[Fe/H]>$ (2)	$([Fe/H]_c)_{uv}$ (3)	$([Fe/H]_c)_{Mg_2}$ (4)	R_{eff} (5)	$\log\sigma_0$ (km/s) (6)
2768	+0.046	+0.263	+0.041	64.1	2.277
2974	+0.082	+0.403	+0.242	24.4	2.359
3115	+0.126	+0.399	+0.314	32.2	2.424
3193	+0.032	+0.297	+0.202	26.7	2.313
3377	-0.211	+0.055	+0.000	34.4	2.135
3379	+0.136	+0.322	+0.306	35.3	2.313
3605	-0.170	+0.061	-0.457	21.2	1.995
3607	+0.008	+0.238	+0.266	43.4	2.336
3608	-0.007	+0.287	+0.338	33.7	2.310
3610	-0.109	+0.070	-0.104	15.4	2.215
3613	+0.017	+0.284	+0.073	27.4	2.336
3640	-0.018	+0.172	-0.055	32.2	2.267
3872	+0.120	+0.304	+0.386	18.1	2.408
4125	+0.030	+0.378	+0.202	58.5	2.380
4261	+0.222	+0.530	+0.483	36.1	2.500
4278	-0.096	+0.183	+0.169	34.4	2.402
4283	-0.003	+0.280	-0.015	12.5	2.123
4365	+0.152	+0.392	+0.410	49.8	2.429
4374	+0.048	+0.255	+0.282	50.1	2.473
4387	-0.042	+0.097	-0.240	15.7	2.069
4406	-0.008	+0.318	+0.330	94.9	2.407
4472	+0.180	+0.473	+0.290	104.0	2.484
4473	-0.025	+0.221	+0.274	26.1	2.280
4478	-0.145	+0.120	-0.135	13.4	2.183
4486	+0.125	+0.538	+0.403	94.9	2.545
4494	-0.071	+0.149	+0.041	48.7	2.199
4550	-0.167	+0.195	-	15.0	1.903
4551	+0.030	+0.154	-0.047	13.1	2.067
4552	+0.135	+0.412	+0.435	29.3	2.422
4564	-0.035	+0.296	+0.411	19.8	2.225
4621	+0.102	+0.425	+0.467	40.5	2.389
4636	-0.010	+0.436	+0.330	88.5	2.325
4649	+0.240	+0.500	+0.547	68.7	2.535
5322	-0.071	+0.179	+0.049	33.7	2.380
5576	-0.137	+0.068	-0.135	18.1	2.291
5813	+0.028	+0.201	+0.306	57.2	2.377
5831	-0.070	+0.144	+0.153	25.5	2.164
5846	+0.196	+0.458	+0.410	62.7	2.398
5866	-0.094	+0.262	-	40.5	2.153
5982	-0.011	+0.174	+0.210	23.8	2.399

3.1.2. The case of other colors

From the colors for each model collected in Table 2, linear relations similar to (2) are readily derived. The slopes are

$\Delta_{\rm [Fe/H]} = 3.33 \cdot \Delta_{\rm B-V}$,

$\Delta_{\rm [Fe/H]} = 2.30 \cdot \Delta_{\rm B-R}$,

$\Delta_{\rm [Fe/H]} = 3.63 \cdot \Delta_{\rm V-I}$.

These colors are twice or thrice less sensitive to metallicity than U−V. Considering the distributions of color gradients given in Paper I, the mean [Fe/H] gradients are estimated to be 0.24 from B−V, 0.22 from B−R or V−I, *in fair agreement with the value of 0.26 derived from U−V gradients.* The same is true of the range (and dispersion) of [Fe/H] values, central or average, through our sample of galaxies (see below). The calculated B−V, B−R and V−I are in general redder for their assumed U−V: these theoretical deviations from the color-color relations translate into differences in the estimated [Fe/H], ranging from 0.25 dex for B−V up to O.41 dex for B−R. In this connection note that uncertainties in the calculated colors of old stellar populations have been discussed by Charlot et al., 1996. In the following we accept as reliable the [Fe/H] values derived from the U−V data, because of the built-in property of our models, i.e. to agree with the CMR as plotted from observed and calculated U−V colors (see Fig. 1).

3.2. Metallicities distribution

– *Mean metallicities derived from colors*, according to Table 3, are in the range $-0.21 < [Fe/H] < +0.24$, corresponding respectively to NGC 3377 and NGC 4649. Figure 2 shows the mean metallicity distribution derived for our sample, characterized by an average value (and dispersion) of $<$ [Fe/H] $>$ = 0.01±0.11. Central values are about 0.28 dex higher with nearly the same dispersion.
This relatively narrow metallicity range agrees with the results by Gonzáles & Gorgas (1996) and TFWG. The later determine ages and metallicities from a set of 3 line indices, taking into account non-solar chemical compositions: the average of their "central" metallicities for 12 objects in common with our sample (considering their favoured Model 4) roughly agrees with our values from the U−V color, respectively 0.22 with $\sigma = 0.14$ for them, instead of 0.31 with $\sigma = 0.16$ for us. Part of the difference comes from the fact that we use colors at $r = 1.5''$ while they use indices averaged within $r = R_{eff}/8$. In fact, replacing our "central colors" by values integrated within $r = R_{eff}/8$ we recover a mean of 0.265 with $\sigma = 0.13$.
In KA99 mean metallicities are derived from line indices and their gradients, no allowance being made for non-solar compositions. The quoted interval is -0.8 to +0.3. The mean sample value for 20 objects with $<$ [Fe/H] $>$ measured from Mg_2 or Mg_b is -0.13 with $\sigma = 0.22$ that is 0.14 lower than our result, and with a larger dispersion. Note that in KA99, metallicities estimated from the $<$ Fe $>$ index are much lower than from the Mg indices, explaining the large range of mean metallicities in KA99.
– *The well known Faber & Jackson (1976) relation*, between the luminosity (mass) and the central velocity dispersion, can be translated into a metallicity - σ_0 relation. In Figure 3 we plot central metallicities derived from the U−V colors against central velocity dispersions. These quantities are clearly correlated and a least-squares fit gives

$$[\mathrm{Fe/H}]_{\mathrm{C}} = -1.457 + 0.715 \cdot \log \sigma_C \pm 0.097 \qquad (6)$$

with a correlation coefficient of 0.74 . A correlation of similar robustness is found if mean instead of central metallicities are used, reinforcing the idea that the mass-metallicity relation of ellipticals holds for the whole stellar population and not only for the central regions. These rather good correlations also show that metallicities derived from our color data are not affected with large random errors.

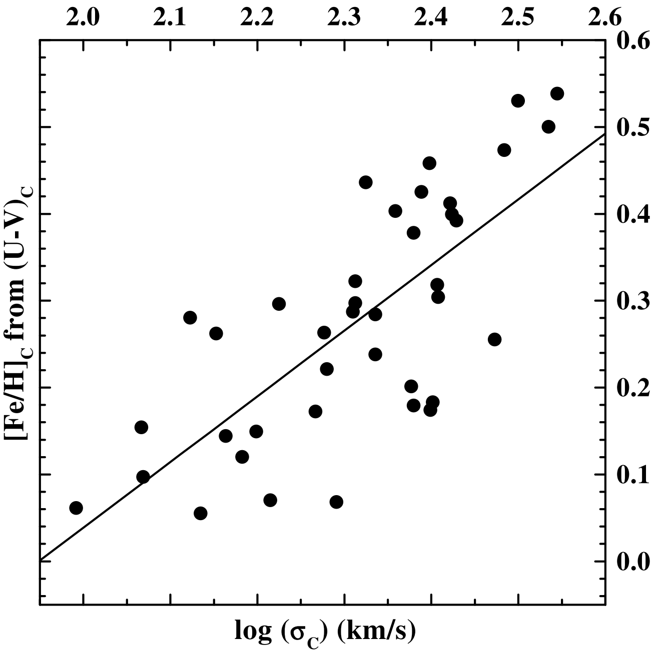

Fig. 3. Central metallicities derived from central colors, as a function of central dispersion velocities

– *How would these results be modified by using SSP models ?* The integrated color of a given SSP depends on the total metallicity Z and thus, systems with nonsolar abundance ratios may have different iron content for the same Z. Therefore, the conversion of [Fe/H] into Z (and vice-versa) requires necessarily the knowledge of abundance ratios at the moment the system forms out of the interstellar medium. In our multi-population approach, since the time evolution of iron and other elements are followed, the integrated properties of the galaxy can be calculated self-consistently. Having in mind these problems, an SSP with an age and metallicity equal to the mean values of the stellar population of a galaxy, will be slightly *redder*. For instance, a globular cluster with parameters comparable to our galaxian model 1 would have a color U−V≈ 1.33 instead of 1.19. Therefore, for a given color (and age), the use of SSPs for the calibration will lead to underestimates of the metallicity.

4. Discussion

In order to check the above derived metallicities and the internal consistency of the series of populations models used for the calibration, we now consider the line indices.

1. *Comparison with metallicities from the Mg_2 index.*
We have computed central metallicities using the Mg_2 index, whose central values were taken from Davies et

al. (1987). The relation [Fe/H]-Mg_2 can be obtained from the results given in Tables 1 and 2, namely

$$[\mathrm{Fe/H}] = -2.17 + 8.04 \cdot \mathrm{Mg}_2 \quad (7)$$

It should be emphasized that this calibration was obtained in the framework of models constituted by a population mix with ages ranging from 12 to 13 Gyr (the more luminous galaxies have a population mix slightly older) and *non-solar* abundances. Central metallicities computed from this equation are given in the fourth column of Table 3. Incidentally, NGC 4486 has a low measured central Mg_2 index, but the profile shows a central drop probably produced by "dilution" of the stellar continuum (see, for instance, Terlevich et al. 1990) occasioned by the central blue object associated to the optical jet. We have adopted for this galaxy a central value Mg_2 = 0.32, obtained from an extrapolation of the radial profile by Davidge (1992), when computing the central metallicity.

Figure 4 compares *central metallicities* resulting from U−V colors with those resulting from Mg_2 line strengths. The good correlation between both determinations was expected (correlation coefficient equal to 0.81), since a robust correlation exists between the central U−V colors and the central Mg_2 indices (Paper I). The mean sample difference is $[\mathrm{Fe/H}]_{\mathrm{U-V}} - [\mathrm{Fe/H}]_{\mathrm{Mg}_2}$ = 0.076±0.120 (rmsd), indicating a rather small systematic difference. The dispersion of about 0.12 dex could result largely from observational errors. On the other hand, the slope of the correlation deviates clearly from the expected one of unity. The [Fe/H] for faint galaxies as derived from Mg_2 tend to be too low, as compared to the values obtained from U−V: the worse case is NGC 3605 (already with a rather low measured Mg_2 index). This systematic disagreement may be somehow related to the calibration procedure summarized in Equations (2) and (6).

The comparison of our results with *average metallicities* derived from line strength gradients is more uncertain, since only 13 galaxies in our sample have measured Mg_2 gradients. Average metallicities were computed for these 13 galaxies, using the same procedure as above, and Mg_2 index gradients from KA99. The mean difference between color and index metallicities is $< [\mathrm{Fe/H}]_{\mathrm{U-V}} > - < [\mathrm{Fe/H}] >_{\mathrm{Mg}_2}$ = +0.13±0.14 (rmsd). The off-set as well as the dispersion are comparable to the values found in the analysis of central metallicities.

2. *The Mg_2 gradient* can be predicted from the $\Delta_{\mathrm{U-V}}$ colour gradient and the calibration relations (2) and (6). The result is $\Delta_{\mathrm{Mg}_2} \approx$ -0.032 which should be compared to the mean sample value derived from the compilation in KA99, namely $\Delta_{\mathrm{Mg}_2} = -0.052\pm0.019$ (rmsd). Only 13 objects in common between KA99 and our sample are used in this comparison, but the distribution for the complete KA99 sample is practically the same. The difference between the predicted and observed mean gradients is possibly larger than allowed by observational errors, and may reflect calibration problems, i.e. inaccuracies in the relations between various colors and spectral indices. The source of the discrepancy is clearly the same as found above in comparing the distributions of central metallicities in our sample of objects.
3. *If the Hβ index is considered*, do we still get a consistent picture ? This index is mainly sensitive to the stellar temperature and hence to age effects, but a weak dependence on metallicity was found by Idiart & de Freitas Pacheco (1995) from the analysis of stars included in their spectral library, basis of our population synthesis code. Our calibration procedure assumes that the population mix throughout E-galaxies has a small age spread. Variations of the star formation efficiency along the radius introduce a metallicity gradient and consequently radial effects on the blanketing, which should reduce the Hβ strength in the inner regions. In fact, most ellipticals display a flat or a positive gradient in Hβ, qualitatively consistent with expectations. From a quantitative point of view, the Hβ gradient can be predicted from the U−V colour gradient and the slope of the Hβ–(U−V) relation: from Table 2, this is equal to -1.105. Combining this with the mean sample gradient in the U−V color given in the previous section, the predicted line strength gradient of the Hβ index is approximately +0.25. The average Hβ gradient derived from data compiled in KA99 is $\Delta_{H\beta}$ = +0.33±0.37 (rmsd), compatible with our prediction in spite of the large spread in the observed values.

Using a linear relation between the U−V color and the Hβ index readily derived from Table 2, we can predict the later from the observed color and compare the predicted values to the observed ones. For this comparison, we used 12 objects in common to our sample and TFWG. Since TFWG give "central" indices averaged in an aperture of $R_{eff}/8$ we obtained from our data average colors relevant to the same galaxy area. The results are given in Table 4. Observed and predicted values are rather well correlated: the mean O-C is 0.04 with σ = 0.18. The slope of the regression may be smaller than 1, but the small number of objects and the large dispersion preclude a firm conclusion. Two galaxies only, i.e. NGC3377 and 5831, have much stronger observed Hβ indices than predicted, which was interpreted by TFWG as due to a young age of the equivalent SSP, circa 3-4 Gyr. The U−V colors of the objects fail to confirm this explanation: according to Worthey, 1994, an SSP of solar metallicity and an age of 3 Gyrs would be 0.30 bluer in U−V than measured in the fiducial aperture $R_{eff}/8$ for the two objects in question.

Altogether, the present check suggests that our evolutive models are able to represent the Hβ indices without

Table 4. Hβ indices: predicted and observed. Observed values are from TFWG. The predictions use our colors in the same aperture and a linear relation from our models (Table 2).

NGC	Hβ (predicted)	Hβ (observed)
3377	1.69	2.09
3379	1.49	1.62
3608	1.58	1.69
4261	1.45	1.34
4374	1.64	1.35
4472	1.63	1.51
4478	1.87	1.84
4552	1.54	1.47
4649	1.46	1.40
5813	1.61	1.42
5831	1.68	2.00
5846	1.50	1.45

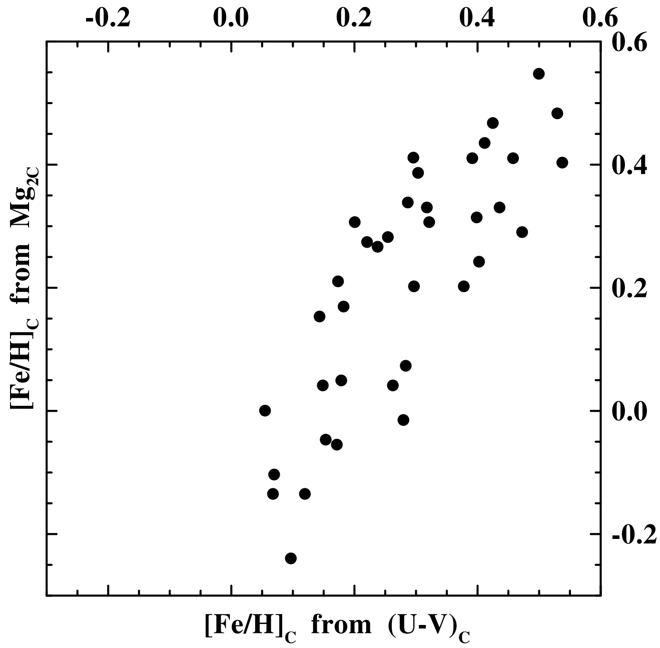

Fig. 4. Comparison between central metallicities derived from colors and line strength indices (Mg_2)

introducing ad hoc age differences between E-galaxies populations.

It is worth mentioning that other effects than age may affect the Hβ strength. De Freitas Pacheco & Barbuy (1995) and de Freitas Pacheco (1997b) have shown that the Hβ strength in globular clusters depends on the horizontal branch morphology. Globular clusters with extended blue tails have larger Hβ indices. These clusters have also dense cores and the blue tails could be a consequence of dynamical effects on stellar evolution (Fusi-Pecci et al. 1993). These effects might contribute to mask the properties of the general stellar population.

5. Conclusions

- From color gradient data presented in Paper I and a color –metallicity calibration described in this work (Sect. 2), we derived a mean metallicity gradient for ellipticals Δ[Fe/H]=-0.26$\pm$0.08. We calculated central and mean metallicities from the U$-$V colors for 40 early-type objects. Our analysis indicates that ellipticals have mean metallicities of about the solar value, but some objects may have near center values as high as three times solar (NGC 4261, NGC 4486, NGC 4649 are examples).
- The derived mean and central metallicities are correlated with central velocity dispersions, an expected result if the CMR is essentially a metallicity sequence.
- On the other hand we calculated the central and mean metallicities from the Mg_2 index and an index–metallicity calibration derived from the same set of population models. The results appear to be in reasonable agreement (Fig. 4), although a systematic difference in the distributions requires further study. Similarly, there are non trivial differences between the observed Mg_2 gradients and the values predicted from the U$-$V gradients.
- We have predicted Hβ indices, using the metallicities derived from the U$-$V colors plus our evolutive models, and compared these with observed data taken from TFWG. For the 12 galaxies in common, the agreement is good (Table 4). *It appears that our grid of model galaxies with an unique age of 15 Gyr is consistent with this set of data.* This is at variance with the interpretation in terms of SSP with large age variations.

Acknowledgements. TPI acknowledges a Fapesp pos-doc fellowship n° 97/13083-7.

References

Borges A.C., Idiart T.P., de Freitas Pacheco J.A., Thévenin F., 1995, AJ 110, 2408
Bower R.G., Lucey J.R., Ellis R.S., 1992a, MNRAS 254, 589
Bower R.G., Lucey J.R., Ellis R.S., 1992b, MNRAS 254, 601
Bressan A., Chiosi C., Tantalo R., 1996, A&A 311, 425
Carlberg R.G., 1984, ApJ 286, 403
Carollo C.M., Danziger I.J., Buson L., 1993, MNRAS 2665, 553
Charlot S., Worthey G., Bressan A., 1996, ApJ 457, 625
Chiosi C., Bressan A., Portinari L., Tantalo R., 1998, A&A 339, 355
Davies R.L., Burstein D., Dressler A., Faber S.M., Lynden-Bell D., Terlevich R.J., Wegner G., 1987, ApJS 64, 581
Davies R.L., Sadler E.M., Peletier R.F., 1993, MNRAS 262, 650
Davidge T.J., 1992, AJ 103, 1512
de Freitas Pacheco J.A., Barbuy B., 1995, A&A 302, 718

de Freitas Pacheco J.A., 1996, RevMexAA Conf. Ser. 4, p.51
de Freitas Pacheco J.A., 1997a, A&A 319, 394
de Freitas Pacheco J.A., 1997b in Abundance Profiles: Diagnostic Tools for Galaxy History, eds. D. Friedli, M. Edmunds, C. Robert, L. Drissen, ASP Conf. Ser. 147, p.205
de Freitas Pacheco J.A., Barbuy B., Idiart T.P., 1998, A&A 332, 19
Faber S.M., Jackson R.E., 1976, ApJ 204, 668
Faber S.M., 1977, in The Evolution of Galaxies and Stellar Populations, eds. B.M. Tinsley, R.B. Larson, Yale University Press, p.157
Faber S.M., Friel E.D., Burstein D., Gaskell C.M., 1985, ApJS 57, 711
Fisher D., Franx M., Illingworth G., 1995, ApJ 448, 119
Franx M., Illingworth G., Heckman T., 1989, AJ 98, 538
Fusi-Pecci F., Ferraro F.R., Bellazini M., Djorgovski S., Piotto G., Buonanno R., 1993, AJ 105, 1145
Gibson B.K., 1997, MNRAS 290, 471
Goudfrooij P., Hansen L., Jorgensen H.E., Nϕrgaard-Nielsen H.U., de Jong T., van den Hoek L.B., 1994, A&AS 104, 179
Gonzáles J.J., Gorgas J., 1996, in ASP Conference Series 86, Fresh Views of Elliptical Galaxies, eds. A. Buzzoni, A. Renzini, A. Serrano, p. 225
Idiart T.P., de Freitas Pacheco J.A., 1995, AJ 109, 2218
Idiart T.P., de Freitas Pacheco J.A., Costa R.D.D., 1996, AJ 112, 254
Idiart T.P., Michard R., de Freitas Pacheco J.A., 2002, A&A 383, 30 (Paper I)
Kodama T., Arimoto N., 1997, A&A 320, 41
Kobayashi C., Arimoto N., 1999, ApJ 527, 573 (KA99)
Larson R.B., 1974, MNRAS 166, 585
Larson R.B., 1975, MNRAS 173, 671
Matteucci F., Tornambè A., 1987, A&A 185, 51
Matteucci F., 1994, A&A 288, 57
Matteucci F. Ponzone R., Gibson B.K., 1998, A&A 335, 855
Michard R., 1998a, A&A 334, 453
Michard R., 1998b, A&A 335, 479
Michard R., 2000, A&A 360, 85
Michard R., 2002, A&A in press
Peletier R.F., Davies R.L., Illingworth G., Davies L., Cawson M., 1990, AJ 100, 1091
Saglia R.P., Maraston C., Greggio L., Bender R., Ziegler B., 2000, A&A 360, 911
Tamura N., Kobayashi C., Arimoto N., Kodama T., Ohta K., 2000, AJ 119, 2134
Tantalo R., Chiosi C., Bressan A., 1998, A&A 333, 419
Terlevich R., Davies R.L., Faber S.M., Burstein D., 1981, MNRAS 196, 381
Terlevich E., Díaz A.I., Terlevich R., 1990, MNRAS 242, 271
Trager S.C., Faber S.M., Worthey G., Gonzáles J.J., 2000, ApJ 119, 1645 (TFWG)
Visvanathan N., Sandage A., 1977, ApJ 216, 214
White S.D., 1980, MNRAS 191, 1P
Worthey G., 1994, ApJS 95, 107
Worthey G., 1996, in Fresh Views of Elliptical Galaxies, eds. A. Buzzoni, A. Renzini, A. Serrano, ASP Conf. Ser. 86, p. 203
Yoshii Y., Arimoto N., 1987, A&A 188, 13